

## Trapped antiprotons produced by cosmic rays in the Earth's magnetosphere

G. Pugacheva<sup>a,\*</sup>, A.A. Gusev<sup>b,c</sup>, U.B. Jayanthi<sup>b</sup>, N.G. Schuch<sup>a</sup>,  
W.N. Spjeldvik<sup>d</sup>, K.T. Choque<sup>b</sup>

<sup>a</sup> Southern Regional Space Research Center, INPE, Av. dos Astronautas 1758, Predio CEA, Caixa Postal 515,  
12201-970 Sao Jose dos Campos, SP, Santa Maria, Brazil

<sup>b</sup> National Institute for Space Research, INPE, Sao Jose dos Campos, Brazil

<sup>c</sup> Space Research Institute of Russian Academy of Science, Moscow, Russia

<sup>d</sup> Weber State University, Ogden, Utah, USA

Received 30 December 2002; received in revised form 8 March 2004; accepted 10 March 2004

### Abstract

The existence of significant fluxes of antiparticles in the Earth magnetosphere has been predicted on theoretical considerations in this article. These antiparticles (positrons or antiprotons) at several hundred kilometers of altitudes, we believe are not of direct extraterrestrial origin, but are the natural products of nuclear reactions of the high energy primary cosmic rays (CR) and trapped protons (TP) confined in the terrestrial radiation belt, with the constituents of terrestrial atmosphere. Extraterrestrial positrons and antiprotons born in nuclear reactions of the same CR particles passing through only 5–7 g/cm<sup>2</sup> of interstellar matter, exhibit lower fluxes compared to the antiprotons born at hundreds of g/cm<sup>2</sup> in the atmosphere, which when confined in the magnetic field of the Earth (in any other planet), get accumulated. We present the results of the computations of the antiproton fluxes at 10 MeV to several GeV energies due to CR particle interactions with the matter in the interstellar space, and also with the residual atmosphere at altitudes of ~1000 km over the Earth's surface. The estimates show that the magnetospheric antiproton fluxes are greater by two orders of magnitude compared to the extraterrestrial fluxes measured at energies <1–2 GeV.

© 2004 COSPAR. Published by Elsevier Ltd. All rights reserved.

**Keywords:** Antiprotons; Cosmic rays; Earth's magnetosphere; Trapped particles

### 1. Introduction

All measurements of the interstellar antiproton spectrum support the idea of their secondary origin, i.e., they are produced by the primary cosmic rays (CR) in nuclear reactions with the interstellar matter, when the CR particles move chaotically in the galactic magnetic fields during their lifetime in the Galaxy. The same nuclear reactions of cosmic ray protons that occur in interstellar media can happen in the Earth's atmosphere, especially in the uppermost residual atmosphere corre-

sponding to high altitudes. In these nuclear reactions a great variety of secondary particles are produced, including the secondary antiprotons. Part of the secondary particles born in the confinement region of the magnetosphere will be trapped in the Earth's vicinity by geomagnetic field creating an antiproton radiation belt around the Earth. This belt is a product of the nuclear reactions similarly to the positron and isotope radiation belts (Gusev et al., 2001; Spjeldvik et al., 1998) created at the altitudes of about 10<sup>3</sup> km above the Earth. The estimates of the trapped antiproton fluxes at these altitudes in the equatorial region, where the atmospheric density is very small ( $\approx 5 \times 10^{-18}$ – $10^{-17}$  g/cm<sup>3</sup>) are obtained. Population of the antiprotons beneath the confinement region was considered by Huang et al. (2001).

\* Corresponding author. Tel.: +55-12-3945-7203; fax: +55-12-3945-6811.

E-mail address: [galina@das.inpe.br](mailto:galina@das.inpe.br) (G. Pugacheva).

2. Antiproton flux production

The minimum proton kinematic energy for the production of an antiproton in the reaction  $pp \rightarrow ppp \bar{p}$  is a threshold energy  $E_{th} = 6m_p = 5629.2$  MeV on the hydrogen target and in  $pA$  reaction  $E_{th} = (2 + 4/A)m_p$  (Gaisser and Levy, 1974). We consider here mostly an antiproton production by the cosmic ray protons. The CR helium nuclei contribute about  $\sim 25\%$  into antiproton production (Jones et al., 2001).

For the modeling of the nuclear reaction products, their spectra, and angular distributions, the nuclear reaction computer code SHIELD (Dementyev and Sobolevsky, 1999) was used. The kinetic energy region of the projectile from several MeV to hundreds of GeV can serve as input in the code for targets with atomic mass  $A \geq 1$ . The simulations were performed to obtain spectra of secondary antiprotons and antineutrons with energies of 1 MeV–1000 GeV in reactions of projectile protons with energies of 6–1000 GeV against target nuclei of hydrogen, helium and oxygen. Fig. 1 shows the mean multiplicity of antiprotons produced in  $(p,p)$ ,  $(p,He)$  and  $(p,O)$  nuclear reactions and its dependence on the projectile proton energy. The multiplicity sharply increases by several orders beyond the threshold kinetic energy of  $\sim 10$  GeV for H, and  $\sim 8$ –9 GeV for He and O, in qualitative agreement with the expression ( $E_{th} = (2 + 4/A)m_p$ ). The multiplicity is practically independent of the target atomic number and is greater for the antineutrons. The resulting angle distribution is very narrow in the cone of  $\approx 5^\circ$  around the incident proton velocity vector, in the laboratory system, for various proton energies for all the targets. Fig. 2 shows the inelastic cross-section values,  $\sigma_{inel}$ , for  $(p,p)$ ,  $(p,He)$ , and  $(p,O)$  reactions obtained by SHIELD code which are in a good agreement with the formulae by Letaw et al. (1983) for  $(p,He)$  and  $(p,O)$  reactions and by Tan and Ng (1982) for  $pp$  reaction.

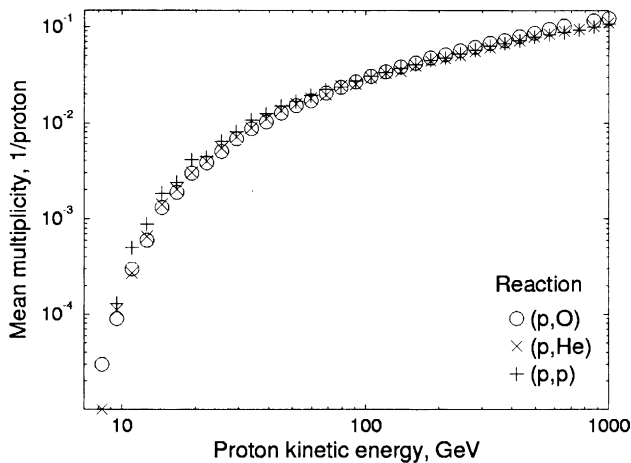


Fig. 1. The number of antiprotons born by one proton in collision with the nuclei of O, He or/and H targets.

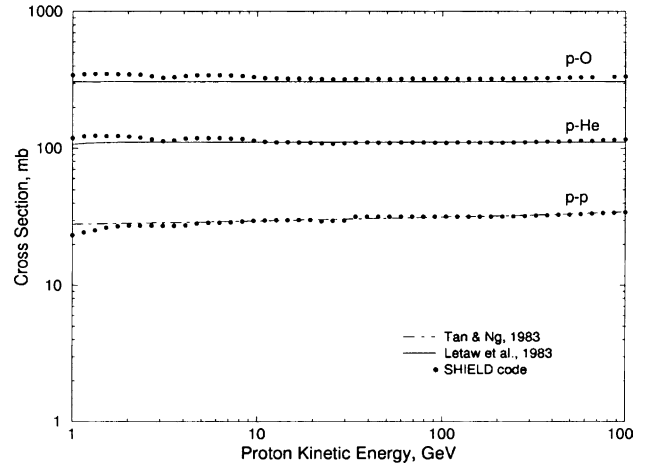


Fig. 2. The cross section of inelastic nuclear reaction of the proton with O, He and H targets versus proton energy.

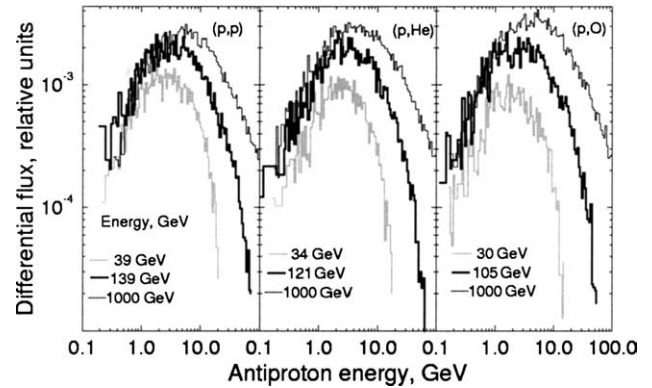


Fig. 3. The differential spectra of the secondary antiprotons born by the proton of given energy on H, He and O targets.

Fig. 3 gives the examples of the differential secondary antiproton production spectra in  $4\pi$  solid angle for different proton energies  $E_p$  on H, He and O target nuclei. The energy distributions at  $E_p \approx 30$  GeV exhibit the characteristic flat maximum between antiproton energies of 1–2 GeV as observed in the various experiments (Arfken, 1985), which indicates the secondary nature of the antiprotons observed. These also attest the secondary antiproton spectrum calculations performed with SHIELD code. The heavier the target nucleus, the more abundant are antiprotons at  $< 200$  MeV energy. The elemental composition of interstellar matter for H, He and O is in the proportion  $1:0.1:10^{-3}$  (Simon et al., 1998) compared to 1.43:29.8:68.76 of the atmosphere at  $L = 1.2$  (the MSIS86 atmospheric model averaged over confinement region with the characteristic parameter  $L = 1.2$ ). Thus, the interstellar antiproton spectrum will have lower contribution at  $< 200$  MeV due to the H target as compared to the atmospheric origin antiproton spectrum with most target atoms of O. The antiproton

production spectrum  $Q_{\bar{p}}(E_{\bar{p}})$ , from the CR proton spectrum ( $dN/dE_p$ ) is obtained by numerical integration of the antiproton production spectra at different proton energies ( $q(E_{\bar{p}}, E_p)$ ) over the CR spectra:

$$Q_{\bar{p}}(E_{\bar{p}}) = \xi \int_{E_{p,th}}^{\infty} q(E_{\bar{p}}, E_p) \frac{dN}{dE_p} dE_p. \quad (1)$$

Here  $\xi$  is a heavy nuclei correction factor of about 1.25 (Jones et al., 2001) describing mostly antiproton input of the CR helium spectrum.

The CR proton spectrum from the balloon experiment CAPRICE (Boezio et al., 1999) was utilized:

$$\frac{dN}{dE_p} = (1.1 \pm 0.11) \times 10^{-4} E_p^{-2.73 \pm 0.06} \quad (m^2 \cdot sr \cdot s \cdot GeV)^{-1}$$

for  $E_p > 20$  GeV. (2)

As far as the spectrum was modulated by solar activity it was demodulated to get the interstellar spectrum:

$$\frac{dN}{dR} = (2.72 \pm 0.02) \times 10^4 R^{-2.928 \pm 0.004} \quad (m^2 \cdot sr \cdot s \cdot GeV)^{-1}$$

for  $R = 1.7 - 200$  GeV. (3)

A solar modulation effect on CR proton flux is appreciable, about 8.7% even at rigidity of 50 GeV, corresponding to the mean kinetic energy of CR proton spectrum above 20 GeV ( $E_p = 47.39$  GeV).

### 3. Interstellar antiproton flux

In computing the interstellar antiproton production spectrum according to Eq. (1) we utilized the interstellar proton spectrum of Eq. (3) and to get the atmospheric one, we used CR proton spectrum modulated by the solar activity, Eq. (2). Multiplying the integral (1) by factor  $\sigma_{inel} N_A / A$  that takes into account the elemental composition of interstellar space and the atmospheric matter, we obtain individually the interstellar and the atmospheric antiproton production spectra per  $g/cm^2$  of the matter (Fig. 4). For the interstellar production spectrum we also take into account the secondary antineutrons, because during their long residence time of  $\sim 10^7$  years in the Galaxy, they decay into antiprotons as the lifetime is short ( $\tau_{lifetime} = 887 \pm 2$  s). However, the magnetospheric antineutrons leave the confinement region sooner and decay outside: even a 10 MeV antineutron travels a distance of  $7R_E$  in the first instant after production. The magnetospheric antiproton production spectrum is more abundant for lower energy antiprotons (Fig. 4). The interstellar antiproton flux is defined by a continuity equation related to the leaky-box model, Eqs. (4), (5).

$$\frac{F_{\bar{p}}(E_{\bar{p}})}{\lambda_{esc}} + \frac{F_{\bar{p}}(E_{\bar{p}})}{\lambda_{inel}} + \frac{d}{dE_{\bar{p}}} \left( F_{\bar{p}}(E_{\bar{p}}) \frac{dE_{\bar{p}}}{dx} (E_{\bar{p}}) \right) = Q(E_{\bar{p}}) + Q_3(E_{\bar{p}}), \quad (4)$$

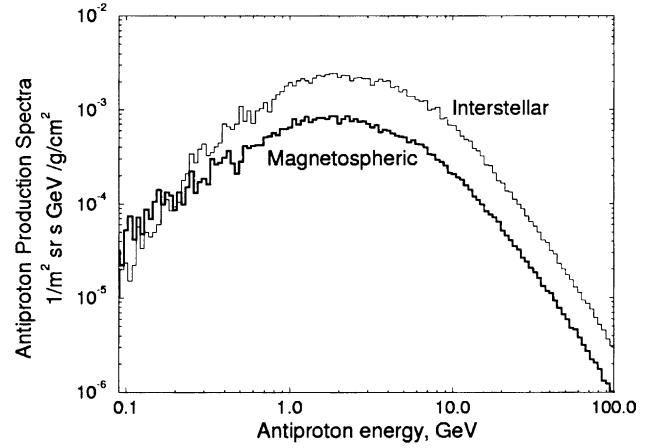


Fig. 4. The spectra of antiprotons born in the  $1 g/cm^2$  of matter by the cosmic ray protons and helium nuclei in the interstellar media and in the inner magnetosphere.

$$Q_3(E_{\bar{p}}) = \frac{N}{A} \int_0^{\infty} \sigma_{inel\bar{p}}(E_{\bar{p}}, E'_{\bar{p}}) F_{\bar{p}}(E'_{\bar{p}}) dE'_{\bar{p}} \quad (5)$$

Here  $\lambda_{esc}$  is escape length of antiprotons in the Galaxy (Jones et al., 2001);  $\lambda_{inel} = A/\sigma_{inel} N_A$  is the antiproton interaction length calculated with the SHIELD-code, the third term describes the antiproton ionization energy losses,  $Q(E_{\bar{p}})$  is the antiproton production spectrum computed above, the function  $Q_3(E_{\bar{p}})$  is a production spectrum of tertiary antiprotons of energy  $E_{\bar{p}}$  produced by all the secondary ones in interactions with the interstellar matter. The Eq. (4) was solved using an iteration procedure with the Runge–Kutta method (Arfken, 1985). A zero approximation accounting only a production of the secondary antiprotons (i.e., with  $Q_3(E_{\bar{p}}) \equiv 0$ ) is depicted in Fig. 5. The contribution of the various interstellar processes and parameters is demonstrated in Fig. 5: for example if the antiproton nuclear

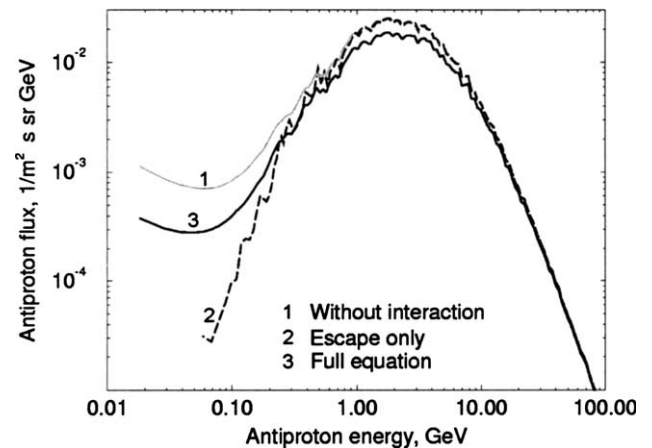


Fig. 5. The computed interstellar antiproton flux without the tertiary component: 1 – without nuclear interactions; 2 – with only escape; 3 – with nuclear interactions, ionization losses and escaping.

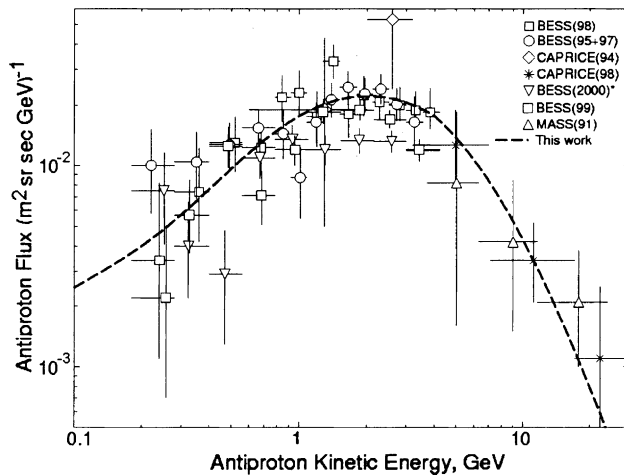


Fig. 6. Comparison of computed galactic antiproton flux and measured one from Boezio et al. (2001) and references therein.

interactions are not accounted (curve 1; Eq. (4) without the second term of left hand is solved); the antiproton nuclear interactions and ionization losses are not accounted (curve 2; Eq. (4) without the second and the third terms of left hand is solved), all processes are included (curve 3; Eq. (4) is solved with all three terms of left hand). In Fig. 6 the computed interstellar antiproton fluxes are presented together with the results of the recent balloon experiments. The experimental and modeling results are in satisfactory agreement; however we did not account a solar modulation and inelastic scattering of the antiproton flux during its life time in the Galaxy.

#### 4. The Earth's antiproton radiation belt

Convinced by good agreement between the simulated and measured galactic antiproton flux we adopted the same approach to compute the magnetospheric trapped antiproton flux at  $L = 1.2$  (i.e., at a mean altitude of  $0.2R_E$  over the Earth surface) in the equatorial region where the maxims of other energetic species such as  $\sim 1$  GeV protons of the albedo origin, positrons, etc., are located. The trapped particles at  $L = 1.2$  possess a narrow pitch-angle distribution around  $90 \pm 20^\circ$ . Thus, approximately all CR nuclei incident at  $L = 1.2$  within the angles around  $\pm 20^\circ$  in relation to the equatorial plane produce antiprotons which will be trapped.

The particles are considered as trapped forever in an ideal magnetic dipole when the gyration radius  $R_L$  around a given magnetic field line is less than  $R_c/10$ , where  $R_c$  is the radius of curvature of the magnetic field line ( $R_c = R_E \times L/3$  at the equatorial region (Chirikov, 1978)). The antiprotons participate in the adiabatic motion in the magnetosphere, drifting on the same L-shell of 1.2 around the Earth, accumulated in magnetic

cavity until ionization losses and nuclear interactions remove them. They could be captured forever in the absence of those losses. From the criteria  $R_c/R_L \geq 10$ , we estimate that antiprotons that could be trapped at  $L = 1.2$  have a maximum kinetic energy of  $E_{crit} = 1.0$  GeV. The particles with greater  $R_L$  have a limited lifetime in the confinement region due to chaotic pitch-angle scattering process described by Chirikov (1978). In Pugacheva et al. (1996) we estimated a particle lifetime  $\tau_{esc}$  at the given L-shell due to this process; a corresponding escape length  $\lambda_{esc} = v\rho\tau_{esc}$  here  $v$  is an antiproton velocity and  $\rho$  is the atmospheric density at  $L = 1.2$ , noted in Section 1. The atmospheric interaction length  $\lambda_{intr}$  and the antiproton ionization losses in the atmosphere will be different of the same for interstellar media due to the difference in the elemental composition. The stopping power values,  $dE_{\bar{p}}/dx$ , for different materials were obtained from American Institute of Standards site <http://physics.nist.gov/PhysRef>). For the trapped magnetospheric antiproton flux modeling we use the same Eq. (4) with the parameters corresponding to the atmospheric elemental composition. The magnetospheric antiproton production spectrum shown in Fig. 4 was utilized. The computed antiproton flux, magnetospherically trapped in the radiation belt, is compared with the interstellar flux in Fig. 7.

The magnetospheric antiproton flux exhibits a soft spectrum which sharply falls to zero at  $\sim E_{crit}$ . At energies lower than 1–2 GeV the magnetospheric trapped antiproton fluxes are about 50–100 times greater than the interstellar fluxes. The same way as in Fig. 5 a contribution of the various processes is demonstrated in Fig. 7: for example when all processes are included (curve 1; Eq. (4) with three terms of left hand is solved), the antiproton escaping from magnetosphere is not

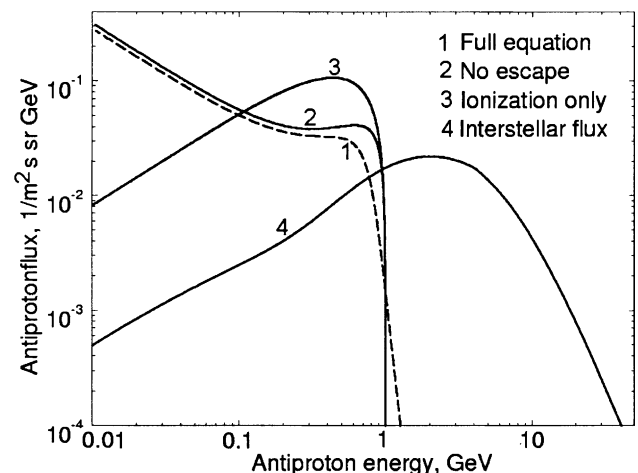


Fig. 7. The computed antiproton flux trapped at  $L = 1.2$ : 1 – with ionization losses, nuclear interactions and escaping; 2 – with ionization losses and nuclear interactions; 3 – with only ionization losses; 4 – the interstellar antiproton flux.

accounted (curve 2; Eq. (4) without the first term of left hand is solved); the nuclear interactions are not accounted (curve 3; Eq. (4) without the first and second terms of left hand is solved) and the interstellar flux is shown by curve 4.

## 5. Conclusion

The modeling considered here for the production of antiprotons utilized nuclear interactions between cosmic ray nuclei with energies above the reaction threshold of 5.6 GeV and the constituents of the environment. Initially, we proceeded with the production of antiprotons in interstellar space and compared with the balloon measurements. In the next step, we calculated the antiproton contribution due to the same cosmic ray nuclei interactions with the atmospheric constituents H, He and O species at altitudes of  $L = 1.2$ , in the near Earth environment to examine the viability of the formation of an antiproton belt and obtain fluxes greater by factors 50–100 at energies  $< 1$  GeV compared to interstellar fluxes. However, during strong geomagnetic storms the trapped radiation can be scattered into lower atmospheric altitudes of the same L-shells and dislocate to other L-shells, that could possibly contaminate interstellar flux measurements. The model estimates of the antiproton fluxes for the inner magnetosphere can be verified in the near future by the new AMS experiment which is scheduled for the installation on the International Space Station for antiparticle – antimatter measurements (The AMS Collaboration, 2000). Besides, experiments on board LEO satellites can monitor the interstellar antiproton flux at high latitudes and the magnetospheric antiproton fluxes at the low latitudes in their orbits.

## Acknowledgements

Dr. A. Gusev thanks CNPq for the fellowships; Dr. Galina acknowledges the support from FAPERGS.

K. Choque thanks the CNPq for Master Science grant.

## References

- Arfken, G. In: *Mathematical Methods for Physicists*, third ed. Academic Press, Orlando, FL, pp. 492–493, 1985.
- Boezio, M., Carlson, P., Francke, T., et al. The cosmic ray proton and helium spectra between 0.4 and 200 GV. *Astrophys. J.* 518, 457–472, 1999.
- Boezio, M., Ambriola, M., Bartalucci S., et al. High-energy cosmic-ray antiprotons with the CAPRICE98 experiment, in: *Proceedings of the 27th International Cosmic Ray Conference*, Humburg, Germany, OG1.1, vol. 5, p. 1695, 2001.
- Chirikov, B.V. The stability problem of charge particle motion in magnetic trap. *Sov. J. Plasma Phys.* 4, 289, 1978.
- Dementyev, A.V., Sobolevsky, N.M. SHIELD-Universal Monte Carlo Hadron transport code: scope and applications. *Radiat. Measur.* 30, 553, 1999.
- Gaisser, T.K., Levy, E.N. Astrophysical implications of cosmic ray antiprotons. *Phys. Rev. D* 10, 1731–1735, 1974.
- Gusev, A.A., Jayanthi, U.B., Pugacheva, G.I., Spjeldvik, W.N. *J. Geophys. Res. A* 106 (11), 26111, 2001.
- Jones, F.C., Lukasiak, A., Ptuskin, V.S. The modified weighted Slab technique: models and results. *Astrophys. J.* 547, 264–271, 2001.
- Huang, C.Y., Derome, L., Buenerd, M. Atmospheric antiprotons, in: *Proceedings of the 27th International Cosmic Ray Conference*, Hamburg, Germany, vol. 5, p. 1707, 2001.
- Letaw, J.R., Silberberg, R., Tsao, C.H. Proton nucleus total inelastic cross sections, an empirical formula for  $E > 10$  MeV. *Astrophys. J. Suppl. Ser.* 51, 271–275, 1983.
- Pugacheva, G.I., Gusev, A.A., Martin, I.M., et al. On the chaos and stability problem in the trapping of anomalous cosmic ray heavy ions by the Earth's magnetosphere. *Planet. Space Sci.* 44, 267–271, 1996.
- Simon, M., Molharan, A., Roesler, S. A new calculations of the interstellar secondary cosmic ray antiprotons. *Astrophys. J.* 499, 250, 1998.
- Spjeldvik, W.N., Pugacheva, G.I., Gusev, A.A., et al. Hydrogen and helium isotope inner radiation belts in the Earth's magnetosphere. *Ann. Geophys.* 16, 931–939, 1998.
- Tan, L.C., Ng, L.K. Parametrization of pbar invariant cross-section in p–p collisions using a new scaling variable. *Phys. Rev. D* 26, 1179–1182, 1982.
- The AMS collaboration. Protons in Near Earth Orbit. *Phys. Lett. B* 472, p. 215, 2000.